Biogas productivity of anaerobic digestion process is governed by a core bacterial microbiota

Tao, Yu; Ersahin, Mustafa Evren; Ghasimi, Dara S.M.; Ozgun, Hale; Wang, Haoyu; Zhang, Xuedong; Guo, Miao; Yang, Yunfeng; Stuckey, David C.; van Lier, Jules B.

DOI
10.1016/j.cej.2019.122425

Publication date
2020

Document Version
Final published version

Published in
Chemical Engineering Journal

Chemical Engineering Journal 380 (2020) 122425

Contents lists available at ScienceDirect

Chemical Engineering Journal

journal homepage: www.elsevier.com/locate/cej

Biogas productivity of anaerobic digestion process is governed by a core bacterial microbiota

Yu Tao[a,b], Mustafa Evren Ersahin[b,c,1], Dara S.M. Ghasimi[b,d,1], Hale Ozgun[b,c,1], Haoyu Wang[b,e,1], Xuedong Zhang[b,1], Miao Guo[a], Yunfeng Yang[f], David C. Stuckey[a,*], Jules B. van Lier[b]

[a] Department of Chemical Engineering, Imperial College London, South Kensington Campus, London SW7 2AZ, UK
[b] Department of Water Management, Section Sanitary Engineering, Delft University of Technology, Delft 2600 GA, The Netherlands
[c] Environmental Engineering Department, Civil Engineering Faculty, Istanbul Technical University, Ayazaga Campus, Maslak, Istanbul 34469, Turkey
[d] Department of Civil Engineering, University of Kurdistan Hewlêr (UKH), Erbil, Kurdistan Region, Iraq
[e] State Key Laboratory of Urban Water Resource and Environment, Harbin Institute of Technology, Harbin 150090, PR China
[f] State Key Joint Laboratory of Environment Simulation and Pollution Control, School of Environment, Tsinghua University, Beijing 100084, PR China

HIGHLIGHTS

- A microbiota-functionality nexus is revealed by 138 samples out of 20 AD reactors.
- A core bacterial microbiota prevailed across all the six types of AD reactors.
- The core bacterial microbiota strongly correlates with the biogas productivity.
- The analysis of a decomplexified OTU network shows apparent community divergence.
- The AD microbiotas are neither functionally redundant or plastic.

GRAPHICAL ABSTRACT

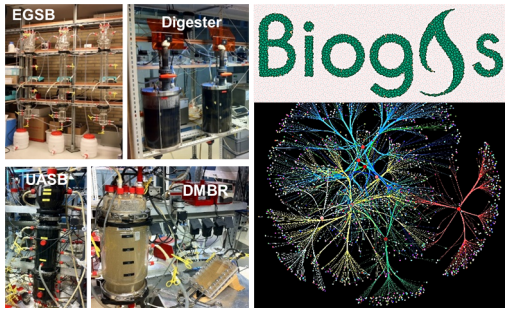

ARTICLE INFO

Keywords:
Anaerobic digestion
Bioreactor
Biogas
Microbiota

ABSTRACT

Anaerobic digestion (AD) has been commercially operated worldwide in full scale as a resource recovery technology underpinning a circular economy. However, problems such as a long start-up time, or system instability, have been reported in response to operational shocks. These issues are usually linked to the dynamics of the functional microbiota in AD. Exploring the microbiota-functionality nexus (MFN) could be pivotal to understand the reasons behind these difficulties, and hence improving AD performance. Here we present a systematic MFN study based on 138 samples taken from 20 well-profiled lab-scale AD reactors operated for up to two years. All the reactors were operated in the same lab within the same period of time using the same methodology to harvest physio-chemical and molecular data, including key monitoring parameters, qPCR, and 16S sequencing results. The results showed a core bacterial microbiota prevailing in all reactor types, including *Bacillus*, *Clostridium*, *Bacteroides*, *Eubacterium*, *Cytophaga*, *Anaerophaga*, and *Syntrophomonas*, while various methanogens dominated different communities due to different inocula origins, reactor temperatures, or salinity levels. This core bacterial microbiota well correlated with biogas production (Pearson correlation coefficient of

Abbreviations: AD, anaerobic digestion; END, the anaerobic digesters treating enzymatically pre-treated bio-solids; EGSB, expanded granular sludge bed; DAnMBR, dynamic anaerobic membrane bio-reactor; UASB, upflow anaerobic sludge blanket; HSD, the anaerobic digesters treating high-salinity wastes; FSD, the anaerobic digesters treating sewage fine sieved fraction; OLR, organic loading rate; SLR, sludge loading rate; sCOD, soluble chemical oxygen demand; SMA, specific methanogenic activity; PBS, phosphate buffer saline

* Corresponding author.
E-mail address: d.stuckey@imperial.ac.uk (D.C. Stuckey).
[1] These authors contributed equally to this work.

https://doi.org/10.1016/j.cej.2019.122425
Received 21 May 2019; Received in revised form 2 August 2019; Accepted 4 August 2019
Available online 05 August 2019
1385-8947/

0.481, $p < 0.0001$). Such strong correlation was even comparable to that between the biogas production and the methanogenic 16S rRNA gene content (Pearson correlation coefficient of 0.481, $p < 0.0001$). The results indicated that AD performance only modestly correlated with microbial diversity, a key governing factor. AD microbiota was neither functionally redundant nor plastic, and a high variety in communities can exhibit a strong difference in reactor performance. Our study demonstrates the importance of a core bacterial microbiota in AD and supports inspiring considerations for design, bioaugmentation, and operational strategies of AD reactors in the future.

1. Introduction

Anaerobic digestion (AD) has been widely acknowledged as an effective biochemical route for the conversion of organic solid wastes and wastewater into energy and valuable products. As a resource recovery technology underpinning a circular economy [1], AD has been operated commercially worldwide in full scale for many decades. However, some commercial AD facilities are reported to suffer from long start-up times, or system instability in response to operational shocks, or even process failure. These issues highlight the need to understand the biological processes underlying AD performance in more depth. An AD reactor can host complex synergistic interactions that are carried out by four functional guilds; namely hydrolysis, acidogenesis, acetogenesis, and methanogenesis [2]. The balance between each microbial group is critical to the efficiency and stability of AD reactors [3–5]. While the microbial assemblies and population dynamics for a single reactor type have been extensively investigated with interesting results [4,6], a comparison across a wide range of reactor configurations is lacking in the literature. Furthermore, the impact of different substrates and inoculating biomass on the performance and stability of different reactor configurations has also not been fully understood yet.

AD performance usually relies on its microbiota's functional redundancy [7,8], the buffer capacity of a community to maintain AD performance in the face of environmental changes by substituting species that perform similar roles [9]. Another different concept is functional plasticity, which is the capacity of a community to accommodate environmental changes by adjusting the metabolic priorities of dominant taxa [10]. A metaproteomic study revealed strong functional redundancy within the AD microbiota, where different microbial guilds carried out the same functions under different temperatures [7]. However, no consistent conclusions have been reached on microbial functionality within research on single AD reactor types, especially under selective pressures, e.g., high temperature, high salinity, or treating recalcitrant substrates. Another ecological factor that determines AD performance is the core microbiota, which refers to the persistent and abundant microorganisms shared across multiple habitats [11]. The existence of core microbiotas in full-scale AD facilities has been postulated before [12], while some researchers have argued that it is difficult to define a single core microbiota among full-scale reactors [13]. However, what is clear is that the governing power of a core microbiota to AD performance is still poorly understood.

In this study, we explored MFN in AD with a specific focus on how can a core bacterial microbiota contribute to AD performance. Since lab-scale anaerobic reactors are ideal habitats for AD microbiota as their functionality can be profiled by measuring intermediate and terminal products straightforwardly and reliably, 20 lab-scale AD reactors with four different configurations were operated for up to two years. They were inoculated with different sources of seed sludge and fed with municipal or industrial substrates in the forms of wastewater or bio-solids. Some key parameters, e.g., chemical oxygen demand (COD), volatile suspended solid (VSS), sludge retention time (SRT), organic loading rate (OLR), and specific methanogenic activity (SMA), were monitored, as well as the intermediate and terminal products, such as biogas and volatile fatty acids. A total of 138 biomass samples were obtained for both qPCR and barcode pyrosequencing analysis to determine their taxonomic diversities. The dataset generated that contained both phylogenetic and performance information was statistically analysed with the aim of understanding MFN that may help researchers develop a proactive management strategy for AD in the future.

2. Material and methods

Twenty lab-scale reactors were operated in the same lab for up to two years. The details of these reactors are summarised in Table 1, including the reactor descriptions, the substrate types, the inoculum sources, the number of biomass samples for sequencing, and the days of operation for each reactor type. More information about the descriptions of each biomass sample and the reactor performance on each sampling day is shown in the Supplementary Data 1.

2.1. Expanded granular sludge bed (EGSB)

Three identical EGSB reactors with a working volume of 3.8 L were operated at 35 ± 1 °C. Internal recycling of the bulk liquid maintained a constant upflow velocity of 8 m/h, and the pH was maintained above 6.9 by adding 0.1 mM NaOH when necessary. LabVIEW software was used to monitor the feed pumps, and to collect online data for pH, ammonia, ORP, and biogas flow. One of the three EGSBs was connected to a 1.8 L pre-acidification bottle, where the raw wet brewery spent grain (BSG) hydrolysate (substrate) was firstly fed, and the pre-fermented liquor was then pumped into the EGSB. The hydraulic retention time (HRT) of the pre-acidification bottle was 8 h, and it was operated under ambient temperatures (18–24 °C). Anaerobic granular sludge from a full-scale upflow anaerobic sludge blanket (UASB, located in Germany) reactor that treated potato-processing wastewater was used to inoculate all the EGSBs, and about 0.2 g volatile suspended solids (VSS) of excess EGSB sludge was dosed as inoculum into the pre-acidification bottle.

Two types of hydrolysate [14] were used as the substrates for the EGSBs; the raw BSG was wet and obtained from a brewery plant, while raw pig manure (PM) was obtained from a manure trader, both in the Netherlands. The enzymatic hydrolysis of BSG and PM was carried out in batch mode to break down the rigid solid matrix and convert the large organic particles into small monomers, and the non-hydrolysed residue was separated from the hydrolysates by filtration. The organic-rich hydrolysate liquor, namely BSG hydrolysate and PM hydrolysate, were used as the substrates. The details of the enzymatic pre-treatment processes are shown in the Supplementary Materials.

2.2. Upflow anaerobic sludge blanket (UASB)

Two identical glass UASB systems with a volume of 7 L were used to treat low-strength synthetic wastewater. Firstly, a stand-alone UASB was operated under different upflow velocities at 25 °C for about 120 days, and a velocity of 1.2 m/h was proven suitable for the next-stage study [15]. After this time, each UASB was connected to an external cross-flow tubular membrane module (X-Flow type, Pentair Inc., USA) so that its effluent could be polished further. The two UASBs were then operated at ambient temperature (25 °C) and low temperature (15 °C). The inoculum for the UASBs was taken from a pilot-scale UASB-Septic tank reactor in Sneek, The Netherlands, treating concentrated

Table 1
Details of the twenty lab-scale AD reactors.

Reactor type	Vol (L)	Substrate type	Inoculum source	Number of reactors[1]	Number of biomass samples	Days of opera-tion
EGSB	3.8	Untreated or enzymatically hydrolysed and filtered brewer's spent grain (BSG hydrolysate); Untreated or enzymatically hydrolysed and filtered pig manure (PM hydrolysate)	A full-scale UASB reactor in Germany treating potato processing wastes	3 EGSBs receiving BSG + 1 EGSB equipped with pre-acidification, receiving BSG+ 2 EGSBs receiving PM	48	Up to 315 days
UASB	7.0	Synthetic municipal wastewater	A pilot-scale UASB reactor in the Netherlands treating black water	1 UASB equipped with ultrafiltration membrane + 1 UASB equipped with both UF membrane and a pre-digester	37	639 days
Dan-MBR	6.8	High-strength Synthetic organic wastewater	A pilot-scale UASB reactor in the Netherlands treating black water	1 Submerged DAnMBR + 1 External DAnMBR	14	145 days
END	5.0	Raw BSG, suspended BSG hydrolysate, filtered BSG hydrolysate, and PM hydrolysate	A full-scale UASB reactor in Germany treating potato processing wastes	1 CSTR receiving raw BSG + 1 CSTR receiving suspended BSG + 1 CSTR receiving hydrolysed and filtered BSG+ 1 CSTR receiving hydrolysed and filtered PM+ 1 SBR receiving hydrolysed and filtered PM	7	Up to 114 days
FSD	8.0	Sewage fine sieved fraction (SFSF)	A full-scale vertical plug flow reactor in The Netherlands treating food waste	1 thermophilic FSD + 1 mesophilic FSD	22	629 days
HSD	4.0	High salinity brackish recirculation wastes	A full-scale digester from a Dutch marine fish processing factory	3 HSDs	10	361 days

1 The number of reactors for each type, including the same reactor but used during different periods of time, receiving various substrates.

wastewater from toilets (black water). An anaerobic digester with a volume of 7 L was connected to the 15 °C UASB as a side-digestion step, with open recirculation of bulk sludge after the system had been operated for over 500 days. More details were introduced in the Supplementary Materials.

2.3. Dynamic anaerobic membrane bio-reactor (DAnMBR)

Two DAnMBRs were used to treat high-strength synthetic wastewater, and each DAnMBR consisted of a completely mixed digester with a working volume of 7.4 L, and a membrane module with a total filtration area of 0.014 m^2; the module was placed either inside (submerged DAnMBR) or outside (external DAnMBR) the digester. A coarse (average pore size of 10 μm) woven-fabric material made of polypropylene (Lampe BV, the Netherlands) was used to separate large particles from the water and provided the basis for a dynamic biofilm and bio-cake that could reject finer particles in the wastewater [16]. The biogas produced was recycled using a diaphragm pump (N86 KTDCB, KNF, Germany) to mix the bulk liquid in the digesters. The sludge retention time (SRT) was maintained at 20 or 40 days, and the HRT was fixed at 10 days. The temperature was controlled at 35.5 ± 0.4 °C using a water bath, and the inoculum for the DAnMBRs was the same as the one used for inoculating the UASBs. Details about the synthetic wastewater and other operational conditions are given in the Supplementary Materials.

2.4. Digester treating sewage fine sieved fraction (FSD)

Four identical water-jacketed completely-mixed digesters with a working volume of 8 L were used to treat sewage fine sieved fraction (SFSF) in batch mode. The experiment was carried out under both thermophilic (55 °C) and mesophilic (35 °C) conditions, with duplicate reactors at each condition [17]. The inoculum for the thermophilic digesters was obtained from a plug-flow composting digester treating vegetable, fruit, and yard (VFY) wastes, with a dry matter content of about 35% (DRANCO, OWS, Brecht, Belgium). The mesophilic inoculum was taken from an anaerobic digester that treated primary and secondary sludge in a municipal wastewater treatment plant (Harnaschpolder, Delft, The Netherlands), with a maximum solids content of 5%, and an SRT of 22 d. The SFSF was taken from a sewage treatment plant in Blaricum, The Netherlands; raw municipal sewage firstly passed through a 6-mm, coarse screen, and then a 350-μm mesh fine sieve (Salsnes Filter, Norway). The compact fine sieve was implemented as an alternative to primary clarification prior to biological nutrient removal. The SFSF mainly contained toilet paper residues (cellulosic fibres), with some sand, hair, leaves, and an undefined matrix.

2.5. Digester treating high-salinity wastes (HSD)

Three identical completely-mixed glass digesters were used to treat high-salinity wastes, each with a working volume of 4 L, and operated at 35 ± 1 °C. The inoculum was collected from a full-scale digester treating fish-processing wastes in The Netherlands, with a salinity of 17 g/L. The substrate was collected from a 60-μm mesh fine sieve of a brackish recirculation aquaculture system that was located in a turbot fish farm in The Netherlands, and the farming temperature was maintained at about 18 °C. The salinity of the substrate varied within the range of 13–17 g/L, depending on the sampling season [18].

2.6. Digester treating enzymatically pretreated hydrolysates (END)

In total, five identical glass digesters were used to treat raw or pretreated BSG and PM that were discussed previously. Three were operated in continuous mode, treating raw BSG, suspended BSG, and solubilised BSG hydrolysate, while two digesters were operated in batch mode, treating solubilised BSG or PM hydrolysates. Each digester had a working volume of 5 L and was operated at 35 ± 1 °C, with a pH of 7.1–7.7 and an HRT of 10 or 15 days. More information about the END reactor can be found in the Supplementary Materials.

2.7. Organic loading rate (OLR) for AD reactors

The OLRs for the UASBs and DAnMBRs were kept at 2 kg COD/(m^3·d) throughout the entire experiment, while different OLRs were applied to the EGSBs, ENDs, HSDs, and FSDs. The OLRs of the EGSBs varied between 3 and 17 kgCOD/(m^3·d) by changing the dilution rate of the hydrolysates. The OLRs for ENDs, HSDs and FSDs fell into the range of 3–8 kgCOD/(m^3·d), 1–4 kgCOD/(m^3·d), and 2.5–13.5 kgCOD/(m^3·d), respectively. In addition to the classic definition of the parameter OLR with the units of kgCOD/(m^3·d), sludge loading rate (SLR) was also used in this study with the units of kgCOD/(kgVSS·d).

2.8. Chemical analyses

Total suspended solids (TSS), total solids (TS), VSS, and volatile solids (VS) were measured according to standard methods [19]. Chemical oxygen demand (COD), ammonia nitrogen, and total nitrogen were measured by testing kits (product numbers 1145410001, 114559, and 114763, MERCK, Germany) and a spectrophotometer (Spectroquat TR420/NOVA60, MERCK, Germany). The samples for soluble COD measurement were prefiltered through 0.45-μm fibreglass filters (Spartan 30, Whatman, United Kingdom), while salinity was measured using a conductivity meter. Volatile fatty acids (VFAs), including acetic acid, propionic acid, butyric acid, isobutyric acid, valeric acid, and isovaleric acid, were measured by gas chromatography (Agilent HP7890, USA) equipped with a flame ionisation detector and a capillary column (19095 N-123 HP INNOWX). The temperatures of the column, injector port and detector were 70 °C, 250 °C, and 300 °C, respectively, while the carrier gas was nitrogen at a flow rate of 10 mL/min and a split flow of 40 mL/min. Biogas composition was measured using a 7890A gas chromatograph (Agilent HP7890, USA) equipped with a thermal conductivity detector and a 45–60 mesh, matrix molecular sieve 5A column (Sigma–Aldrich, USA), and helium was the carrier gas with a flow rate of 30 mL/min. The temperatures of the injection inlet, oven, and detector were 100 °C, 60 °C, and 105 °C, respectively.

2.9. Specific methanogenic activity (SMA) analyses

SMA assays were used to determine the rate at which methanogenic microorganisms can convert acetate into methane. The SMA test was carried out in triplicate using an Automated Methane Potential Test System (AMPTS, Bioprocess Control, Sweden). Sodium acetate (2 g/L) was the primary carbon source in the synthetic media, while no sodium acetate was added to the medium for the control groups. The ratio of inoculum VSS to substrate COD (I/S) was 2:1, while SMA results were expressed as kgCOD $_{methane}$/(kgVSS·d), allowing for comparisons of results between the different AD reactors. In this paper, the specific methane production rate indicates the volume of methane generated per time unit per mass of biomass, while the methane yield tells the extent of organic matter conversion (total COD) into biomethane. If related to the incoming COD, both SMA and methane yield shows the efficiency of each reactor in producing biogas.

2.10. Biomass sampling, storage, and DNA extraction

Fresh biomass samples were washed with 1 × phosphate buffer saline (PBS) and centrifuged at 7000 × G for 7 min. The supernatant was then discarded, and the pellets were re-washed with 1 × PBS for a second time, followed by centrifugation at 17000 × G for 20 min. The supernatant was discarded, and the pellets were stored at −25 °C for DNA extraction. UltraClean microbial DNA isolation kits (MoBio Laboratories, Inc., USA) were used for DNA extraction as per the manufacturer's protocol, with a minor modification in that twice bead-beating (5 min), and heating (5 min) were applied in sequence to

enhance the lysis of microbial cells. DNA isolation was confirmed by agarose gel electrophoresis, and the concentrations were examined using Nanodrop 1000 equipment (Thermo Scientific, USA).

2.11. 16S rRNA gene sequencing

The sequencing of the 16S rRNA genes was performed in the Research and Testing Laboratory (Lubbock, TX, USA) with the following primers: (1) U515F ('5-GTG YCA GCM GCC GCG GTA A-3′) and U1071R ('5-GAR CTG RCG RCR RCC ATG CA-3′) were used for bacteria and archaea with a high coverage of over 90% for each domain; (2) Arch341F ('5-CCC TAY GGG GYG CAS CAG-3′) and Arch958R ('5-YCC GGC GTT GAM TCC AAT T-3′) were used for archaea. Pyrosequencing was done using a Roche system (454 Life Science, Branford, CT, USA) with Titanium chemistry, and an average of 3000 reads was retrieved from the 138 biomass samples. The sequences have been deposited in the NCBI database under Bioproject PRJNA396877. The Quantitative insights into the microbial ecology (QIIME) pipeline (version 1.8.0) [20] were used for demultiplexing and filtering low quality, chimeric reads. Operational taxonomic units (OTUs) were classified using an open-reference method. The alignment was filtered to remove common gaps with a phylogenetic tree constructed *de novo* using FastTree. The biodiversity analysis was also performed by QIIME.

2.12. Real-time qPCR

A real-time qPCR analysis was performed on an ABI 7500 instrument (USA) with the primer sets of Bac516-F-Bac805-R for bacteria, and ARC787-F-ARC1059-R for archaea. The qPCR amplification was done in a 20-μL reaction, including 10 μL 2 × SGExcel FastSYBR Mixture (With ROX, Sangong Biotech, China), 8.6 μL dH_2O, 0.2 μL each of forward and reverse primers (1 pmol/μL), and 1 μL DNA templates. Molecular grade water was used as a negative control, and triplicate PCR reactions were carried out for all the samples and controls. The thermal cycling program was: 2 min at 50 °C, 1 min at 95 °C, followed by 40 cycles of 10 s at 95 °C, 35 s at X °C (X = 56 for Bac516-F/Bac805-R, X = 61 for ARC787-F/ARC1059-R). Finally, a melting curve analysis was performed to verify the specificity of the PCR products, which was: denaturation of 1 min at 95 °C, cooling of 1 min at 55 °C and then heat till 95 °C again, at a temperature-increase rate of 0.5 °C/cycle. The standard curves were constructed using the mixed DNAs extracted from the biomass that were harvested from all types of AD reactors used in this study. The target 16S rRNA gene sequences were amplified by PCR with the corresponding primer sets and cloned into pGEM-T easy vectors (Sangong Biotech, Shanghai, China). A 10-fold serial dilution series ranging from 10^4 to 10^{10} copies/mL was generated for each plasmid. The slopes of the plasmid standard curves had a mean value of −3.313. The threshold cycle (CT) values determined were plotted against the logarithm of their initial copy numbers. All the standard plasmids and DNA samples were amplified in triplicate.

2.13. Statistical methods

The OTUs networks were constructed using QIIME and visualised by Cytoscape v3.2.0 [21]. The functional redundancy analysis [22] consists of 1-dimensional non-metric multidimensional scaling of two data sets, (i) Bray-Curtis dissimilarities at the OTU level (microbial community structure), and (ii) AD performance indicators, including bioreactor performance (methane production, removal efficiency of soluble COD (sCOD), and VFAs/OLR ratio). The Pearson correlation coefficient analysis was performed using XLSTAT add-in for Microsoft Excel. Two indexes, frequency and occupancy, were introduced to show the prevalence of microorganisms. The frequency (f) is defined as the relative abundance of a particular genus in a given sample (f > 0.1% if a genus owning a relative abundance is higher than 0.1%). The occupancy is defined as the percentage of the total samples (%) satisfying a particular frequency. Details of these two indexes are shown in Section 3.3.

3. Results

3.1. Reactor performance

Among all the reactor types, the EGSBs reached the highest SLR (0.86 kgCOD/(kgVSS·d)) and volumetric methane production (4580 NmL methane/(L·d)), with a relatively high sCOD removal efficiency (60–90%, Fig. 1). No substantial accumulation of VFAs was found in the EGSBs for most days except for; 1) when the OLR of the BSG hydrolysate was rapidly increased from 10 to 16 kgCOD/(m^3·d) within 21 days and; 2) when the OLR of the PM hydrolysate was raised to > 8 kgCOD/(m^3·d). The SMA value of the seed sludge for the EGSBs was 0.7 $kgCOD_{methane}$/(kgVSS·d), while it decreased to 0.4 $kgCOD_{methane}$/(kgVSS·d) for the BSG-fed EGSB sludge, and 0.2 $kgCOD_{methane}$/(kgVSS·d) for the PM-fed EGSB sludge after nearly one-year in operation. Although the same seed sludge and substrates were applied to the EGSBs and ENDs, the applicable OLRs and the methane production of the EGSBs were significantly higher than the ENDs (*t*-test $P = 0.0049$ for OLRs, $P = 0.0024$ for methane production). As expected, the hydrolysate-fed ENDs delivered superior performance compared with the raw BSG-fed ENDs, with about 50% higher methane production. The UASBs and DAnMBRs demonstrated similar methane production and methane yields (Fig. 1c & d), which could be related to the same seed sludge and a fixed OLR of 2 kgCOD/(m^3·d). The DAnMBRs performed well with higher SLRs and delivered a nearly complete removal of sCOD along with the formation of a dynamic cake layer. The FSDs were operated under both thermophilic (55 °C) and mesophilic (35 °C) conditions, and surprisingly, the latter achieved a significantly higher methane yield (280 ± 90 NmL/gCOD) than the former (239 ± 70 NmL/gCOD) ($p < 0.05$, Student test), in which COD represents the added COD. The OLR for the HSD was maintained at a relatively low level in order to avoid toxicity induced by high salinity, yet its methane yield was higher than most other reactors (Fig. 1d).

3.2. Taxonomic diversity

The alpha-diversity level of a community is usually characterised by two indices of richness and evenness [23]. The EGSB communities showed the highest level of both richness and evenness, while similar levels were found in the UASBs, DAnMBRs, and ENDs (Figs. S1, S2), while the FSD microbiota demonstrated the lowest biodiversity. It was intriguing to find high levels of biodiversity in the HSD communities, even though the high salinity substrate was clearly a strong environmental selection factor. Notably, strong immigration of microorganisms from the raw BARS substrate (the substrate for HSDs) was seen as the qPCR results showed a very close correlation between bacterial 16S rRNA gene copy numbers in the substrate and HSD sludge (Fig. S3). Finally, only a modest correlation was observed between the bacterial and archaeal communities in all the reactors (Pearson correlation coefficient of 0.196, $p = 0.021$, Fig. S4).

An OTU network is a graphic way to illustrate connections between microorganisms in complex systems [24]. In our study, if all the OTUs in every reactor were plotted, an overly complex network would be generated (Fig. S5a). Thus, a simplified network is presented without losing key OTUs that play essential roles in maintaining the network's integrity (Fig. S5, S6). It is interesting to note that the centricity of each reactor type (Fig. S7) is similar to the beta-diversity plots (e.g., non-metric multidimensional scaling (NMDS) of the Bray-Curtis distance, Fig. S8), which agrees with recent findings of the advantage of a network-based beta-diversity analysis [25]. The biomass samples from the same reactor types were close to each other and formed a group.

Interestingly, a few early-day DAnMBR and UASB communities were close due to the same origin of their inoculum, while their daughter communities diverged from each other (Fig. S7). The FSD samples were divided into two sub-groups based on the thermophilic or mesophilic conditions of the reactors. Two clusters were observed in the EGSB samples, representing the reactors that were fed with BSG

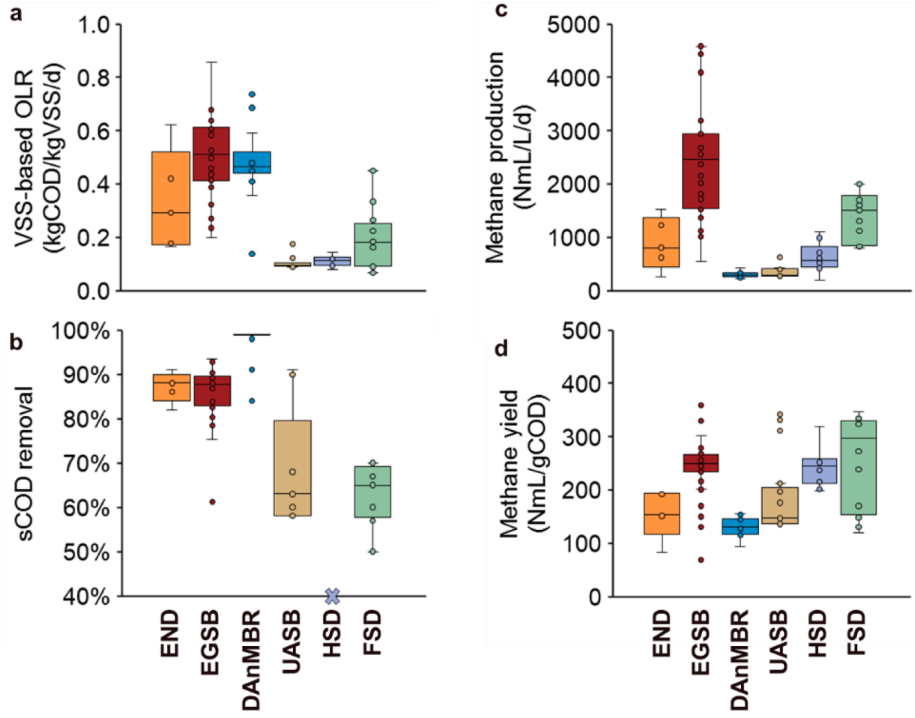

Fig. 1. Box and whisker charts showing AD performance. (a) The applied organic loading rates based on dry biomass concentrations. (b) Soluble COD (sCOD) removal efficiencies. The sCOD removal data of the UASBs did not take into the considerations of UF-membrane filtration, and the data for the HSDs were not available. (c) The volumetric methane production rates measured under standard conditions (STP, 0 °C, 101.325 kPa). (d) Methane yields measured under standard conditions (STP, 0 °C, 101.325 kPa). For each box and whisker chart, the top of the higher whisker shows the maximum number of the group, the top of the box represents the 75th percentile of the group, the line through the box represents the median of the group dataset, the bottom of the box shows the 25th percentile of the sample, while the bottom of the lower whisker represents the minimum number of the group.

hydrolysates or PM hydrolysates, with a few overlapping close to the inoculum. A clear divergence of the inoculum community appeared in the EGSBs and ENDs, which shared the same inocula and substrates. A similar trend in divergence also occurred in the UASB vs. DAnMBR, which showed more overlapped samples but separated groups.

3.3. Prevailing microorganisms

In total, 606,432 counts were retrieved after pyrosequencing all biomass samples (including seed sludge). Also, 50 phyla and 698 genera were clustered. Low evenness across the entire microbial taxa was notable since the top 7 (*Firmicutes*, *Bacteroidetes*, *Proteobacteria*, *Synergistetes*, *Chloroflexi*, *OP9,* and *Euryarchaeota*) out of the 50 phyla accounted for 92% in relative abundance. Over 86% of the genera had an abundance < 0.1% on average, while only 92 had an average abundance > 0.1%. Several bacterial taxa showed high relative abundance across all types of AD reactors, for example, the relative abundance of *Clostridium* was 12% on average, followed by *Cytophaga*, *Bacteroides*, and *Bacillus*, which had an average abundance close to 9% (Fig. 2a).

Besides high abundance, prevalence is another critical feature for microbes. We hypothesise that a prevalent taxon should have a

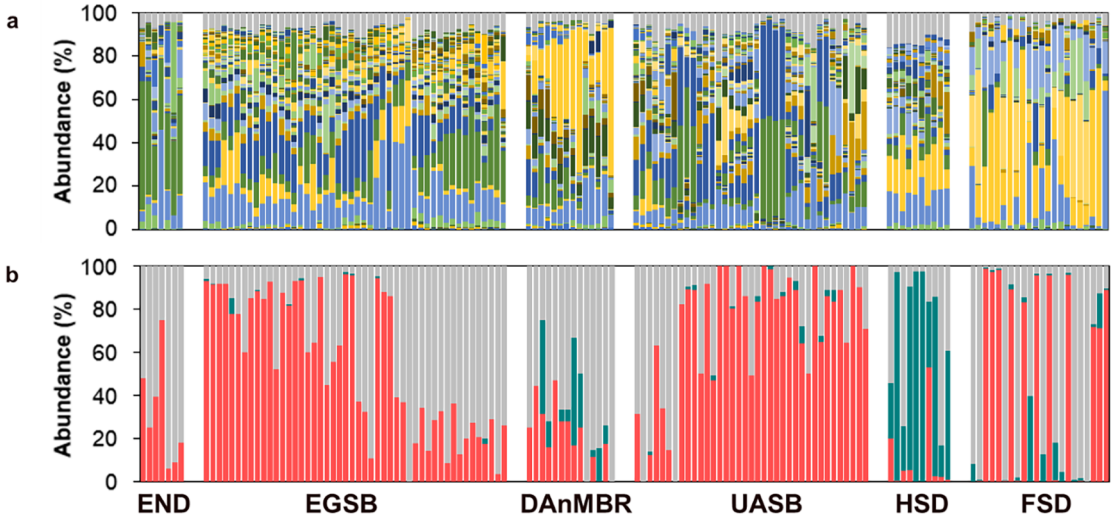

Fig. 2. Bacterial and methanogenic archaea assemblies of all the AD reactors. (a) bacterial communities and only the members of Group 1, 2, and 3 are shown. The taxonomic information of each bacterial genus can be found in the Supplementary Data 2. (b) methanogenic communities, in which acetoclastic methanogens (red bars) refers to the strains that can produce methane via acetic acid (mainly), or methanol and methylamines (occasionally), and all of them belong to the genus *Methanosaeta*. The versatile methanogens (cyan bars) are the strains with a versatile function that can produce methane via multiple sources: acetic acid, hydrogen + carbon dioxide, carbon monoxide, or methanol, methylamines, methylsulfides, methylated compounds + hydrogen. They belong to the genus of *Methanosarcina*. The hydrogenotrophic methanogens (grey bars) produce methane mainly from hydrogen + carbon dioxide, and cannot produce methane from acetic acid or in a versatile way.

relatively high abundance in all types of reactors, regardless of their reactor configuration, inocula, substrate, and environmental conditions. To address this hypothesis, we performed an analysis of prevalence based on two levels. For Level 1, all the 138 samples, independent of reactor type, were categorised based on the genera frequency level (Fig. 3). Taking the genus *Synergistes* as an example, 122 samples were under a frequency of f > 0.1%, and hence the occupancy was 122/138 (88%) at f > 0.1% (Fig. 3). Under such a definition, there were twenty-five genera having an occupancy of over 50% at f > 0.1%, and six with occupancy over 50% at f > 1%. It was striking that *Clostridium* had a high occupancy value of 46% even at f > 10%, demonstrating its dominance in most samples, especially in the PM-hydrolysate-fed EGSB and the thermophilic FSD under high organic loads.

For Level 2, we grouped the genera based on the distributional evenness of a genus in each type of AD reactor. A Group 1 member was defined as a genus appearing at least once in each reactor type with an abundance > 1%, while a Group 2 member represents a genus appearing at least once in each reactor type with an abundance > 0.1% [26]. Group 1 genera include *Bacillus*, *Clostridium*, *Bacteroides*, *Eubacterium*, *Cytophaga*, *Anaerophaga*, and *Syntrophomonas*. We also identified twenty-two Group 2 genera, many of whom were hydrolytic and fermentative bacteria (Fig. 3). Almost all the other 669 OTUs were endemic populations that showed a satellite mode across the entire AD microbiota (Figs. S5, S6).

Euryarchaeota, the phylum that most methanogens belong to with a few exceptions [27], existed in all the reactors but with significant differences in relative abundance, varying from < 0.1% to 30%, and averaging 2.7% (Fig. S9). The EGSB had the highest average abundance of *Euryarchaeota* (6.4 ± 7.2%), followed by the UASB (1.8 ± 1.6%). The DAnMBR and all the other digesters (END, HSD, and FSD) hosted far fewer *Euryarchaeota* (0.025–0.7%), regardless of the same seed sludge and substrate (e.g., EGSB vs. END, UASB vs. DAnMBR). There are three guilds of methanogens based on physiology; (1) acetoclastic methanogens, namely *Methanosaeta*; (2) versatile ones, namely *Methanosarcina*; and (3) the hydrogenotrophic ones, which is a big group of all the other methanogens [28]. Versatile methanogens dominated the HSD microbiota under ammonia-rich (3 g/L) and high salinity (17 g/L) environments. Several samples of the DAnMBRs and thermophilic FSD also had a high abundance of the versatile methanogens. Most EGSB and UASB samples were dominated by acetoclastic methanogens, but they are less in the PM-hydrolysate-fed EGSB that had high levels of ammonia (1.4 g NH_4^+-N/L). The distribution of methanogens in the FSDs varied considerably with different temperatures, i.e., the thermophilic digester was entirely dominated by hydrogenotrophic methanogens, whereas the mesophilic one had a higher relative abundance of acetoclastic methanogens.

3.4. Quantification of microorganisms

No substantial difference was observed in the bacterial and archaeal 16S rRNA gene copy numbers among different reactor types, although different inocula were used, and various configurations were applied (Fig. S10). Most samples had bacterial 16S rRNA gene copy numbers in the range of 10^9-10^{11}/gram VS, except for the two END samples that digested raw BSG and unfiltered BSG hydrolysates. The distribution of archaeal 16S rRNA gene copy numbers ranged from 10^6 to 10^{12} gene copy numbers/gram VS (Fig. S10), indicating a noticeable variation in the number of methanogens, given the fact that methanogens accounted for 95% ± 7% of the archaeal community.

3.5. Microbiota-functionality nexus (MFN)

Since the microbiota is essential for converting organic substrates into methane, we explored the relationship between the microbiota and AD performance. Five parameters were used to characterise performance, namely applied OLR, SLR, sCOD removal efficiency, methane production efficiency, and methane yield (Table 2). Some representative alpha-diversity indices and the relative abundance of critical guilds were used to compare the performance datasets (Table 2). Overall, the statistical analyses suggested a positive linear correlation between AD performance (i.e., methane yield) and the substrate supply (i.e., applied OLR) (R^2 = 0.85, Fig. S11).

Moderate correlations between methane production and archaeal 16S rRNA gene copy numbers (Pearson correlation coefficient 0.481) and methanogen abundance were observed (Pearson correlation

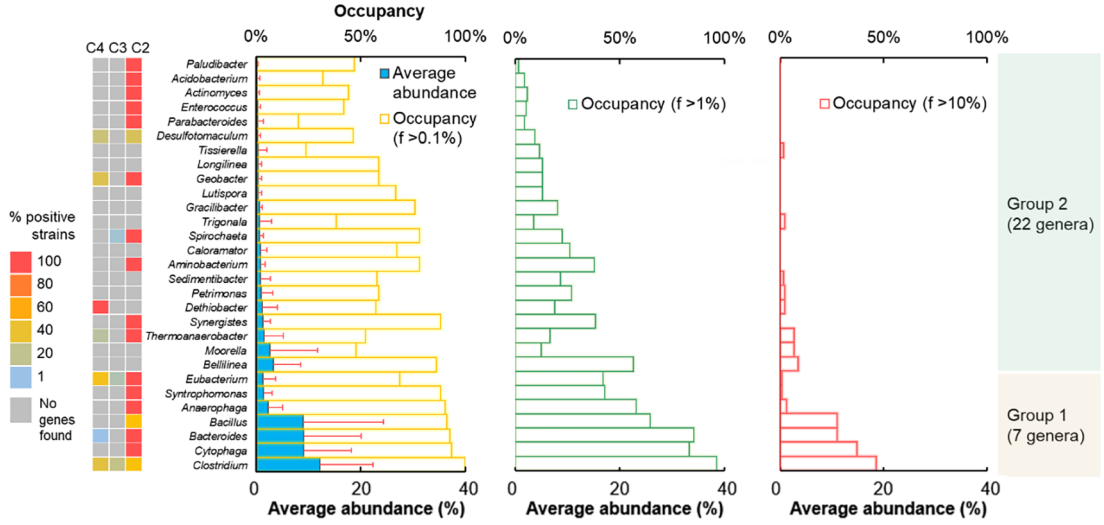

Fig. 3. A core bacterial microbiota across all the AD reactors. Among all of the 698 genera, 92 had an average abundance of over 0.1%, and blue bars highlight the top 29 genera. The error bar represents the standard deviation of each reactor's dataset. A frequency over 0.1% (f > 0.1%) means a situation under which a certain genus has a relative abundance higher than 0.1% in an individual sample. Occupancy is the ratio of the sample number that satisfies a particular frequency to all 138 samples, and it is shown in hollow bars (yellow f > 0.1%, green f > 1%, red f > 10%). Seven genera can be categorised as Group 1 members as at least one reactor of each reactor type once contained such a genus with an abundance > 1%. Twenty-two genera can be categorised as Group 2 members, which means at least one reactor of each type once contained such a genus with the abundance > 0.1%. The other 57 genera are categorised into Group 3 (not shown) as they were not prevalent in all the reactors, but each one was present at a high abundance in a specific reactor type. The heat map on the left illustrates the percentage of VFA-producing strains out of all known strains in each Group 1 or Group 2 genus. C4, C3, C2 represents butyric acid, propionic acid, acetic acid, respectively.

Table 2
Pearson correlation analysis between reactor performance and microbiota indices.

	OLR kgCOD/(m^3·d)	SLR kgCOD/(kgVSS·d)	sCOD removal %	Methane production NmL/(L·d)	Methane yield NmL/gCOD
Richness					
Observed OTUs	0.130	**0.191**	**0.218**	**0.198**	0.142
Margalef	0.165	**0.217**	**0.222**	**0.232**	0.153
Menhinick	**0.284**	**0.287**	**0.200**	**0.344**	**0.191**
ACE	0.158	**0.239**	**0.237**	**0.216**	0.130
Chao1	0.140	**0.234**	**0.229**	**0.205**	0.131
Evenness					
Shannon	**0.294**	**0.281**	0.068	**0.310**	0.067
Simpson	**0.241**	**0.222**	−0.079	**0.213**	−0.040
Brillouin	**0.282**	**0.277**	0.069	**0.298**	0.054
Gini	**−0.291**	**−0.295**	**−0.206**	**−0.354**	**−0.210**
PD	0.144	**0.203**	**0.250**	**0.221**	0.156
qPCR results					
Bacterial 16S gene copies	**−0.284**	**−0.257**	−0.178	**−0.259**	−0.082
Archaeal 16S gene copies	**0.382**	**0.278**	0.195	**0.481**	**0.267**
The abundance of key bacterial guilds					
Syntrophs	0.156	0.172	0.082	0.128	−0.110
VFA Producers	0.061	**0.273**	**0.341**	0.053	−0.009
Group 1	**0.494**	**0.308**	**0.008**	**0.481**	**0.326**
Group 2	−0.065	0.114	**0.210**	−0.044	0.080
Euryarchaeota (Phylum)	**0.366**	**0.320**	0.212	**0.418**	**0.240**

Note: The bold numbers are the values with a p-value < 0.05 (see details in the Supplementary material Table S1).

coefficient 0.418). The same coefficient of 0.481 suggested that the Group 1 members (total relative abundance) and methane production efficiency were also correlated at moderate levels. A stronger relationship between OLR and the Group 1 members (Pearson correlation coefficient of 0.494) was found in comparison with that between OLR and the archaeal 16S rRNA gene copy numbers (Pearson correlation coefficient = 0.382). The alpha diversity indices were not correlated to the performance datasets as strongly as the Group 1 bacteria or methanogens but were at a modest level (coefficient > 0.3 with Menhinick richness, Shannon evenness, and Gini evenness). A statistically significant coefficient of 0.341 was observed between the abundance of VFA producers and sCOD removal, indicating the importance of acidogenesis in sCOD removal.

4. Discussion

4.1. Did functional redundancy govern AD microbiotas?

In nature, greater diversity increases the likelihood that functions will be maintained under stress, which gives the community a higher buffer capacity [9]. Microbial diversity has been suggested to play a critical role in maintaining the functional stability and robustness of AD as it provides a suite of parallel pathways for trophic steps, and a high diversity is often correlated with well-performing AD facilities [5]. However, our results only showed a weak correlation between diversity indices and performance parameters (Table 2).

Contradictory conclusions have been reported in the literature about the contribution of a microbiota's functional redundancy on biogas-producing performance. We found in our reactors that most microbiotas were not strongly governed by functional redundancy, and very few displayed functional plasticity (Fig. 4). The definition of functionality in our study was based on a holistic estimation of AD reactor performance, including biogas productivity, rather than an evaluation based on functional genes via sequencing.

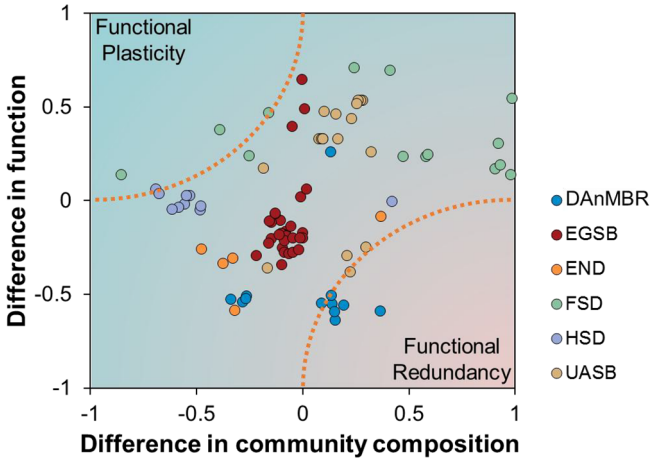

Fig. 4. The community-function relationship. Each point represents a pairwise comparison between the community structure and function. The former is shown on the X-axis as the difference in community composition (1-dimensional non-metric multidimensional scaling of Bray-Curtis dissimilarities at the OTU level). The function is shown on the y-axis as the difference in function (1-dimensional non-metric multidimensional scaling of reactor performances including methane production, sCOD removal efficiency, and VFAs/OLR ratio). The area closer to (−1, 1) indicates high possibilities of functional plasticity, while the zone closer to (1, −1) suggests substantial probabilities of functional redundancy.

4.2. How can a core microbiota contribute to AD performance?

Methanogens are vital players in AD microbiotas. Three types of methanogens, namely acetoclastic, versatile, or hydrogenotrophic methanogens, dominated our AD reactors independently or jointly (Fig. 2b). However, the versatile and hydrogenotrophic methanogens were more likely to be dominant under near-extreme conditions, such as high influent COD concentrations (20,000 mg COD/L in DAnMBRs), high temperature (55 °C in the thermophilic FSD), or high ammonia loading (3000 mg NH_4^+-N/L in an EGSB). Quite a few studies have reported that *Methanosarcina* and some hydrogenotrophic methanogens outcompeted acetoclastic ones under intense selective pressures, such as either high [29] or low [7] temperatures, and high ammonia loading rates [30]. The slow-growing *Methanosaeta* microorganisms (μ_{max} = 0.12 /d, doubling time 5.8 d) have an affinity for acetate of 30 mgCOD/L [2], so they have a kinetic advantage over other types of methanogens when an effluent COD is low, which is pursued in the industry usually.

The Group 1 microbiota are comprised of seven bacterial genera that have a remarkable capacity for both hydrolyzing and fermenting a broad spectrum of organic compounds (Fig. 3). An excellent example of this is the genus *Clostridium*, which topped both average abundance and occupancy in all reactor types; it has been increasingly reported to be very versatile, degrading both proteins and cellulose, and producing VFAs [31]. Also, among all the known 102 stains, 98 are capable of generating acetic acid, 44 can produce propionic acid, and 74 are butyric acid producers (The Short Chain Fatty Acid Database. Center for Microbial Ecology, Michigan State University. http://fungene.cme.msu.edu/scfa/). For these reasons, they are prevalent in a large number of AD systems, especially the ones operating under extreme conditions [32]. *Bacilli* were also highly abundant in our reactors, and many *Bacillus* strains can decompose both fats and carbohydrates [33]. *Cytophaga* is a common cellulolytic bacterium with some members capable of rapidly degrading crystalline cellulose, or cellulose digestion products such as cello-oligosaccharides, cellobiose, or glucose [34]. *Bacteroides* is also a versatile and ubiquitous taxon that was prevalent in AD; it has been commonly reported that *Bacteroides* is not only ubiquitous in natural environments and human bodies but also plays a

significant role in hydrolysing a broad array of polysaccharides and producing fatty acids in AD [35]. *Eubacterium* can degrade complex aromatic acids to produce mixed volatile fatty acids [36], while *Anaerophaga* is also a strictly anaerobic fermentative bacterium [37], both of which are commonly found in AD reactors [38,39].

Syntrophic bacteria had a much lower abundance in our reactors compared with the VFA-producing bacteria (Fig. S12). Although they usually form a relatively small population in AD reactors [40], they are function-specialized and resilient with small genomes that code for unusual metabolic pathways and suggest nutritional self-sufficiency [41]. In our study, *Syntrophomonas* was the only syntrophic bacterium in Group 1, and many strains of it are capable of oxidising propionate and butyrate [42]. *Synergistetes*, a Group 2 member, has been reported to use amino acids and in turn, provide short-chain fatty acids or act as syntrophic acetate oxidizers [12]. Most non-syntrophic Group 2 bacterial genera are capable of acidogenesis and/or acetogenesis except for *Trigonala*, whose function in AD is still unknown (Table S2). Intriguingly, very few Group 2 members are capable of both hydrolysis and fermentation.

4.3. A striking divergence of microbiota in AD reactors

Microbiota divergence appeared commonly in our reactors on both temporal and spatial coordinates. It happens from the mother (seed sludge) to the daughter community, also in different reactor types. Taking the UASB and DAnMBR as examples, they were started with the same seed sludge, and as a consequence, their early-stage biomass samples shared very similar community structures (Fig. S7). However, a clear divergence occurred over the following 1-year of operation as the two groups evolved in very different directions (Fig. S7). Microbiota divergence also occurred in two replicate reactors receiving different substrates (Fig. S13). It is notable that the divergence mentioned above was revealed by the multidimensional scaling of either the sole genomic datasets or the performance parameters (Fig. S8).

Microbial community divergence also occurred at a centimetre or even millimetre scale in our reactors. For example, taxonomic differences appeared in the same submerged DAnMBR between the bulk sludge and cake layer, which had utterly different methanogenic community structures (Fig. S14). Since DAnMBR is a self-forming biofilm-based type of reactor, such divergence might also happen in other biofilm-based processes. Furthermore, the granules in the bottom of the UASBs usually hosted twice as many *Euryarchaeota* than the biomass in the middle or top part. Interestingly, microbiota divergence even happened in a 2 mm-diameter granular sludge between the core layer and surface layer (Fig. S15), in which the surface layer contained 1.1% of *Euryarchaeota,* while the core contained 6.7%. Considering a low residential COD concentration (100–150 mg/L) and relatively large granule size, such divergence might be a function of diffusion and mass transfer [43].

5. Conclusions

In this study, we exploited MFN in AD by combining fully profiled operational parameters with bioinformatics in lab-scale reactors. Our results reveal a weak functional redundancy in AD microbiotas, which indicates the possibility of maintaining excellent performance via manipulating communities. For example, it may worth trying to augment a failing AD facility by adding core microbiotas that can either be the ones confirmed to prevail in a previously satisfying operational period, or the universal strains in AD systems, e.g., from *Clostridium* or *Bacteroides*. While we did not expect to be able to draw firm conclusions here about the controlling power of microbiota on AD performance, our study strongly indicates that a core bacterial microbiota exists in various AD reactors, and its abundance is closely related to the biogas-producing performance. More studies are expected to reveal how multi-dimensional factors rule AD performance in the future.

Acknowledgements

This study was funded by a research grant from the Biotechnology and Biological Sciences Research Council (BBSRC) of the UK (grant number BB/K003240/2). The authors would like to express their gratitude for the Ph.D. Fellowship awards provided by the Turkish Academy of Sciences (TUBA) to HO, by HUYGENS Scholarship Program to MEE.

The authors would like to thank Prof Merle de Kreuk and Prof Henri Spanjers from the Delft University of Technology for guiding the operation of the reactors, and analysing data. The authors would also like to thank Dr. Margarida Temudo and Dr. Margot Schooneveld and their research team at the DSM Biotechnology Center for supplying valuable materials for ENDs.

Availability of research data

Full sequencing data are available online in the NCBI database (https://www.ncbi.nlm.nih.gov/Traces/study/?acc=SRP115101).

Author contributions

YT applied molecular analysis, contributed to the analytical measurement of the samples from the EGSBs, UASBs, and DAnMBRs, and assisted in operating the EGSBs. MEE, DSMG, HO, HW, and XZ contributed equally to this work. They operated the DAnMBRs, FSDs, UASBs, EGSBs, and HSDs, respectively, and measured the parameters of each AD reactor. MG contributed to the microbiota-functionality statistical analysis, while YY, DCS, and JvL raised critical comments and significantly improved the manuscript. All the authors approved the submission of the final-version manuscript.

Declaration of Competing Interest

The authors declare that they have no competing of interests.

Appendix A. Supplementary data

The supplementary material document contains supplementary methods, supplementary tables (Tables S1 and S2), and supplementary figures (Figs. S1–S15). Two separate supplementary data files are also supplied in an Excel format. Supplementary data to this article can be found online at https://doi.org/10.1016/j.cej.2019.122425.

References

[1] W.R. Stahel, The circular economy, Nature 531 (2016) 435–438.
[2] J. van Lier, N. Mahmoud, G. Zeeman, Biological Wastewater Treatment: Principles, Modelling and Design. Chapter 16: Anaerobic Wastewater Treatment. ISBN: 9781843391883 Published by IWA Publishing, London, UK. 2008.
[3] L. Zhang, K. Loh, J. Lim, J. Zhang, Bioinformatics analysis of metagenomics data of biogas-producing microbial communities in anaerobic digesters: a review, Renew. Sust. Energ. Rev. 100 (2019) 110–126.
[4] S.G. Langer, C. Gabris, D. Einfalt, B. Wemheuer, M. Kazda, R.B. Bengelsdorf, Different response of bacteria, archaea and fungi to process parameters in nine full-scale anaerobic digesters, Microb. Biotech. (2019) under press.
[5] J.J. Werner, D. Knights, M.L. Garcia, N.B. Scalfone, S. Smith, K. Yarasheski, et al., Bacterial community structures are unique and resilient in full-scale bioenergy systems, Proc. Natl. Acad. Sci. U.S.A. 108 (2011) 4158–4163.
[6] X. Goux, M. Calusinska, S. Lemaigre, M. Marynowska, M. Klocke, T. Udelhoven, et al., Microbial community dynamics in replicate anaerobic digesters exposed sequentially to increasing organic loading rate, acidosis, and process recovery, Biotechnol. Biofuels 8 (2015) 122.
[7] E. Gunnigle, A. Siggins, C.H. Botting, M. Fuszard, V. O'Flaherty, F. Abram, Low-temperature anaerobic digestion is associated with differential methanogenic protein expression, FEMS Microbiol. Lett. 362 (2015) fnv059.
[8] S.G. Langer, S. Ahmed, D. Einfalt, F.R. Bengelsdorf, M. Kazda, Functionally redundant but dissimilar microbial communities within biogas reactors treating maize silage in co-fermentation with sugar beet silage, Microb. Biotechnol. 8 (2015) 828–836.
[9] T.J. Battin, K. Besemer, M.M. Bengtsson, A.M. Romani, A.I. Packmann, The ecology

and biogeochemistry of stream biofilms, Nat. Rev. Microbiol. 14 (2016) 251–263.
[10] E.M. Morrissey, R.L. Mau, E. Schwartz, T.A. McHugh, P. Dijkstra, B.J. Koch, et al., Bacterial carbon use plasticity, phylogenetic diversity and the priming of soil organic matter, ISME J. 11 (2017) 1890–1899.
[11] C. Astudillo-Garcia, J.J. Bell, N.S. Webster, B. Glasl, J. Jompa, J.M. Montoya, et al., Evaluating the core microbiota in complex communities: a systematic investigation, Environ. Microbiol. 19 (2017) 1450–1462.
[12] D. Riviere, V. Desvignes, E. Pelletier, S. Chaussonnerie, S. Guermazi, J. Weissenbach, et al., Towards the definition of a core of microorganisms involved in anaerobic digestion of sludge, ISME J. 3 (2009) 700–714.
[13] R. Mei, M.K. Nobu, T. Narihiro, K. Kuroda, J. Munoz Sierra, Z. Wu, et al., Operation-driven heterogeneity and overlooked feed-associated populations in global anaerobic digester microbiome, Water Res. 124 (2017) 77–84.
[14] H. Wang, Y. Tao, M. Temudo, M. Schooneveld, H. Bijl, N. Ren, et al., An integrated approach for efficient biomethane production from solid bio-wastes in a compact system, Biotechnol. Biofuels 8 (2015) 62.
[15] H. Ozgun, M.E. Ersahin, Y. Tao, H. Spanjers, J.B. van Lier, Effect of upflow velocity on the effluent membrane fouling potential in membrane coupled upflow anaerobic sludge blanket reactors, Bioresour. Technol. 147 (2013) 285–292.
[16] M.E. Ersahin, Y. Tao, H. Ozgun, H. Spanjers, J.B. van Lier, Characteristics and role of dynamic membrane layer in anaerobic membrane bioreactors, Biotechnol. Bioeng. 113 (2016) 761–771.
[17] D.S.M. Ghasimi, Y. Tao, M. de Kreuk, M.H. Zandvoort, J.B. van Lier, Microbial population dynamics during long-term sludge adaptation of thermophilic and mesophilic sequencing batch digesters treating sewage fine sieved fraction at varying organic loading rates, Biotechnol. Biofuels 8 (2015) 171.
[18] X. Zhang, Y. Tao, J. Hu, G. Liu, H. Spanjers, J.B. van Lier, Biomethanation and microbial community changes in a digester treating sludge from a brackish aquaculture recirculation system, Bioresour. Technol. 214 (2016) 338–347.
[19] APHA. Standard Methods for the Examination of Water and Wastewater, eighteenth edition. American Public Health Association, Washington D.C., USA. 2005.
[20] J.G. Caporaso, J. Kuczynski, J. Stombaugh, K. Bittinger, F.D. Bushman, E.K. Costello, et al., QIIME allows analysis of high-throughput community sequencing data, Nat. Methods 7 (2010) 335–336.
[21] R. Saito, M.E. Smoot, K. Ono, J. Ruscheinski, P.L. Wang, S. Lotia, et al., A travel guide to Cytoscape plugins, Nat. Methods 9 (2012) 1069–1076.
[22] K.G. Peay, P.G. Kennedy, J.M. Talbot, Dimensions of biodiversity in the Earth mycobiome, Nat. Rev. Microbiol. 14 (2016) 434–447.
[23] L. Wittebolle, M. Marzorati, L. Clement, A. Balloi, D. Daffonchio, K. Heylen, et al., Initial community evenness favours functionality under selective stress, Nature 458 (2009) 623–626.
[24] L. Wu, Y. Yang, S. Chen, M. Zhao, Z. Zhu, S. Yang, et al., Long-term successional dynamics of microbial association networks in anaerobic digestion processes, Water Res. 104 (2016) 1–10.
[25] T.S. Schmidt, J.F. Matias Rodrigues, C. von Mering, A family of interaction-adjusted indices of community similarity, ISME J. 11 (2017) 791–807.
[26] J. Cheng, T. Ringel-Kulka, I. Heikamp-de Jong, Y. Ringel, I. Carroll, W.M. de Vos, et al., Discordant temporal development of bacterial phyla and the emergence of core in the fecal microbiota of young children, ISME J. 10 (2016) 1002–1014.
[27] P.N. Evans, D.H. Parks, G.L. Chadwick, S.J. Robbins, V.J. Orphan, S.D. Golding, et al., Methane metabolism in the archaeal phylum Bathyarchaeota revealed by genome-centric metagenomics, Science 350 (2015) 434–438.
[28] R.K. Thauer, A.K. Kaster, H. Seedorf, W. Buckel, R. Hedderich, Methanogenic archaea: ecologically relevant differences in energy conservation, Nat. Rev. Microbiol. 6 (2008) 579–591.
[29] D.S.M. Ghasimi, Y. Tao, M. de Kreuk, B. Abbas, M.H. Zandvoort, J.B. van Lier, Digester performance and microbial community changes in thermophilic and mesophilic sequencing batch reactors fed with the fine sieved fraction of municipal sewage, Water Res. 87 (2015) 483–493.
[30] J. De Vrieze, A.M. Saunders, Y. He, J. Fang, P.H. Nielsen, W. Verstraete, et al., Ammonia and temperature determine potential clustering in the anaerobic digestion microbiome, Water Res. 75 (2015) 312–323.
[31] F. Lu, A. Bize, A. Guillot, V. Monnet, C. Madigou, O. Chapleur, et al., Metaproteomics of cellulose methanisation under thermophilic conditions reveals a surprisingly high proteolytic activity, ISME J. 8 (2014) 88–102.
[32] M. Di Giacomo, M. Paolino, D. Silvestro, G. Vigliotta, F. Imperi, P. Visca, et al., Microbial community structure and dynamics of dark fire-cured tobacco fermentation, Appl. Environ. Microbiol. 73 (2007) 825–837.
[33] M. Carballa, L. Regueiro, J.M. Lema, Microbial management of anaerobic digestion: exploiting the microbiome-functionality nexus, Curr. Opin. Biotechnol. 33C (2015) 103–111.
[34] Y.T. Zhu, L.L. Han, K.L. Hefferon, N.R. Silvaggi, D.B. Wilson, M.J. McBride, Periplasmic Cytophaga hutchinsonii endoglucanases are required for use of crystalline cellulose as the sole source of carbon and energy, Appl. Environ. Microbiol. 82 (2016) 4835–4845.
[35] P.Y. Hong, E. Wheeler, I.K. Cann, R.I. Mackie, Phylogenetic analysis of the fecal microbial community in herbivorous land and marine iguanas of the Galapagos Islands using 16S rRNA-based pyrosequencing, ISME J. 5 (2011) 1461–1470.
[36] G. Qiu, Y.H. Song, P. Zeng, L. Duan, S. Xiao, Characterization of bacterial communities in hybrid upflow anaerobic sludge blanket (UASB)-membrane bioreactor (MBR) process for berberine antibiotic wastewater treatment, Bioresour. Technol. 142C (2013) 52–62.
[37] K. Denger, R. Warthmann, W. Ludwig, B. Schink, Anaerophaga thermohalophila gen. nov., sp nov., a moderately thermohalophilic, strictly anaerobic fermentative bacterium, Int. J. Syst. Evol. Microbiol. 52 (2002) 173–178.
[38] R.M. McKeown, C. Scully, A.M. Enright, F.A. Chinalia, C. Lee, T. Mahony, et al., Psychrophilic methanogenic community development during long-term cultivation of anaerobic granular biofilms, ISME J. 3 (2009) 1231–1242.
[39] S. Yang, H.V. Phan, H. Bustamante, W. Guo, H.H. Ngo, L.D. Nghiem, Effects of shearing on biogas production and microbial community structure during anaerobic digestion with recuperative thickening, Bioresour. Technol. 234 (2017) 439–447.
[40] T. Narihiro, T. Terada, A. Ohashi, Y. Kamagata, K. Nakamura, Y. Sekiguchi, Quantitative detection of previously characterized syntrophic bacteria in anaerobic wastewater treatment systems by sequence-specific rRNA cleavage method, Water Res. 46 (2012) 2167–2175.
[41] M.J. McInerney, J.R. Sieber, R.P. Gunsalus, Syntrophy in anaerobic global carbon cycles, Curr. Opin. Biotechnol. 20 (2009) 623–632.
[42] N. Muller, P. Worm, B. Schink, A.J. Stams, C.M. Plugge, Syntrophic butyrate and propionate oxidation processes: from genomes to reaction mechanisms, Environ. Microbiol. Rep. 2 (2010) 489–499.
[43] J. Dolfing, Kinetics of methane formation by granular sludge at low substrate concentrations – the influence of mass-transfer limitation, Appl. Microbiol. Biotechnol. 22 (1985) 77–81.